Cell, Vol. 97, 635–646, May 28, 1999, Copyright ©1999 by Cell Press

Structural View of the Ran–Importin β Interaction at 2.3 Å Resolution

Ingrid R. Vetter,* Andreas Arndt,* Ulrike Kutay,† Dirk Görlich,† and Alfred Wittinghofer*‡
*Max-Planck-Institut für molekulare Physiologie
Otto Hahn Straße 11
D-44227 Dortmund
Germany
†Zentrum für Molekulare Biologie
Universität Heidelberg
D-69120 Heidelberg
Germany

Summary

Transport receptors of the Importin β family shuttle between the nucleus and cytoplasm and mediate transport of macromolecules through nuclear pore complexes. They interact specifically with the GTP-binding protein Ran, which in turn regulates their interaction with cargo. Here, we report the three-dimensional structure of a complex between Ran bound to the nonhydrolyzable GTP analog GppNHp and a 462-residue fragment from Importin β. The structure of Importin β shows 10 tandem repeats resembling HEAT and Armadillo motifs. They form an irregular crescent, the concave site of which forms the interface with Ran-triphosphate. The importin-binding site of Ran does not overlap with that of the Ran-binding domain of RanBP2.

Introduction

Transport of macromolecules between the nucleus and cytoplasm proceeds through nuclear pore complexes (NPCs) and is largely mediated by shuttling transport receptors of the Importin β superfamily that share an N-terminal RanGTP-binding motif (Fornerod et al., 1997b; Görlich et al., 1997). These receptors interact directly with NPCs and, according to the direction they carry a cargo, can be classified as importins or as exportins.

Productive transport cycles require importins to bind their cargo in the cytoplasm and to release it in the nucleus, whereas exportins have to operate with exactly the opposite preference (for review, see Mattaj and Englmaier, 1998). The RanGTP gradient model (Görlich et al., 1996b) gives a plausible explanation of how this compartment specificity of cargo loading and release can be achieved. Ran is a small Ras-like GTP-binding protein that switches between a GTP- and a GDP-bound form by GTP hydrolysis and nucleotide exchange (Drivas et al., 1990; Bischoff and Ponstingl, 1991b; Melchior et al., 1993; Moore and Blobel, 1993). The conversion of RanGTP into RanGDP is catalyzed by the GTPase-activating protein RanGAP1 (Bischoff et al., 1994; Hillig et al., 1999) and further stimulated by the Ran-binding proteins RanBP1/RanBP2 (Bischoff et al., 1995; Richards et al., 1995). RanGAP, RanBP1, and RanBP2 are all excluded from the nucleus and thus deplete RanGTP from the cytoplasm only. RanGTP is generated from RanGDP by the exchange factor RCC1, which is confined to the nucleus (Ohtsubo et al., 1989; Bischoff and Ponstingl, 1991a; Renault et al., 1998). This differential localization of the regulators of Ran's nucleotide-bound state should thus result in a steep RanGTP gradient across the nuclear envelope with a high concentration in the nucleus and very low levels in the cytoplasm. Transport receptors are RanGTP-binding proteins that respond to the RanGTP gradient by loading and unloading their cargo in the appropriate compartment. Importins bind cargo at low RanGTP levels in the cytoplasm and release it upon encountering RanGTP in the nucleus (Rexach and Blobel, 1995; Görlich et al., 1996c; Izaurralde et al., 1997; Siomi et al., 1997). The importin–RanGTP complexes are then reexported to the cytoplasm where RanGTP is removed, allowing the importins to bind and import the next cargo molecule. This disassembly of the importin–RanGTP complex is accomplished by the concerted action of RanGAP1 and RanBP1 (or RanBP2) and results in the hydrolysis of the Ran-bound GTP (Bischoff and Görlich, 1997; Floer et al., 1997; Lounsbury and Macara, 1997). Binding of substrates to exportins is regulated in a converse manner to importins. They bind their cargoes preferentially in the nucleus, forming a trimeric cargo–exportin–RanGTP complex and release their cargo when RanGTP is hydrolyzed in the cytoplasm (Fornerod et al., 1997a; Kutay et al., 1997a).

Karyopherin β/Importin β (Impβ) is a major mediator of nuclear protein import (Chi et al., 1995; Görlich et al., 1995; Imamoto et al., 1995; Radu et al., 1995). It accomplishes import of proteins that carry a classical nuclear localization sequence (NLS). However, Impβ cannot bind NLS proteins directly, but only through an adaptor, namely Importin α (Impα) (Adam and Adam, 1994; Görlich et al., 1994). Impα binds β through its N-terminal *i*mportin *b*eta–*b*inding (IBB) domain. A fusion protein containing an IBB not only binds to Impβ but is also imported by Impβ, demonstrating that Impβ can also operate as an autonomous import receptor, independently of Impα (Görlich et al., 1996a; Weis et al., 1996). Meanwhile a number of "natural substrates" have been identified that can directly be bound and imported by Impβ. These include ribosomal proteins such as L23a and the HIV Rev protein (Henderson and Percipalle, 1997; Jäkel and Görlich, 1998; Truant and Cullen, 1999). Impβ can also heterodimerize with another Ran-binding transport receptor, namely Importin 7 (RanBP7) to mediate import of histone H1 (Görlich et al., 1997; Jäkel et al., 1999).

RanGTP displaces Impα, directly binding import substrates, or Importin 7 from Impβ and also releases Impβ from certain sites of the NPCs. Such displacements by RanGTP are essential events in each of the various Impβ-mediated transport cycles. As a step to understanding nuclear transport receptor function at atomic

‡To whom correspondence should be addressed (e-mail: alfred.wittinghofer@mpi-dortmund.mpg.de).

Table 1. Crystallographic Analysis

Data Collection	
Resolution (Å)	30–2.3
Observed reflections	354,933
Unique reflections	69,758
Completeness	96.6% to 2.3 Å (93.8% from 2.4–2.3Å)
I/σ	28.1 (8.02 from 2.4–2.3Å)
R_{merge}[a]	3.6%
Refinement	
Resolution (Å)	50.0–2.3
Reflections	60,991
R_{crys}[b]	24.6%
R_{free}	27.2%
Model	
Nonhydrogen atoms	
Protein	9,743
Magnesium ions	2
Nucleotide	65
Water	312
Rms deviation from expected geometry	
Bond lengths (Å)	0.007
Bond angles (°)	1.4
Overall B value (Å^2)	41.6

[a] $R_{merge} = \Sigma_{hkl}\Sigma_i|I_i - \langle I\rangle|/\Sigma_{hkl}\Sigma_i|\langle I\rangle|$, where I_i is the intensity for the ith measurement of an equivalent reflection with indices h,k,l.
[b] $R_{crys} = \Sigma_{hkl}||F_{obs}| - |F_{calc}||/\Sigma_{hkl}|F_{obs}|$, where F_{obs} denotes the observed structure factor amplitude and F_{calc} denotes the structure factor amplitude calculated from the model. Ten percent of the reflections were used to calculate R_{free}.

resolution, we report here the three-dimensional structure of the complex of RanGppNHp with an N-terminal 1–462 residue fragment of human Impβ (Impβ$_N$).

Results and Discussion

Structure Determination

The complex of RanGppNHp with the Impβ$_N$ fragment crystallized in space group $P2_1$. The two complexes in the asymmetric unit (termed A and B hereafter) show systematic differences in their structures. Complex A with better defined N and C termini is chosen as the reference structure, and residue numbers will refer to this complex unless stated otherwise. Likewise, superscripts (e.g., 76^{Ran}) are used to identify residues in the first Ran molecule. Unit cell dimensions are a = 65.7 Å, b = 108.9 Å, c = 114.0 Å, β = 100.6. The crystals diffracted to better than 2.3 Å at 100 K using the BW6 synchrotron beamline at DESY/Hamburg. Heavy atom derivative data were collected at room temperature and yielded one good mercury derivative and several weaker ones (Tables 1 and 2). Noncrystallographic averaging combined with density modification of the initial MIR map allowed positioning of Ran and tracing of most of the backbone of Impβ$_N$. This model was then carefully rigid-body refined into the high-resolution synchrotron data set, and side chains were built in. The final model comprises residues 9–176^{Ran} of both Ran molecules, 2–459 of the first Impβ$_N$, 2–439 of the second Impβ$_N$ molecule, and 312 water molecules. Residues 1–8^{Ran} and 177–216^{Ran} of Ran as well as residues 1 and 460–462 of the first Impβ$_N$ molecule and residues 1 and 440–462 of the second Impβ$_N$ molecule are disordered and have been omitted from the model.

Structure of Importin β

Structure Description

The three-dimensional structure of the Impβ$_N$ fragment is purely α-helical and consists of ten tandemly repeated motifs (Figures 1A–1C). They have a length of 32–61 residues and are formed by two antiparallel helices, A and B, that are connected by an intramotif turn. Repeat 10 is an exception in that the connection forms a short 3^{10} helix. The longest intramotif turn is very acidic. Its sequence and length are highly conserved between Impβ$_N$ from lower and higher eukaryotes, and it is also found in transportin. As detailed below, it is involved in Ran binding. Six of the intermotif connections contain additional helices, in five cases 3^{10} helices. The long connection between repeats 7–8 is formed by the elongated helix B7 (25 residues) and an extra long B7-A8

Table 2. Heavy Atom Derivatives

	PCMBS[a]	UAc	$Au(CN)_4$	CH_3Hg I	SeMet
Major sites	2	2	4	8	2
Minor sites	2	1	—	—	—
PP (acentric)	1.00	0.96	0.89	0.77	0.51
R_{cullis}[b] (acentric)	0.84	0.86	0.86	0.89	0.95
PP (centric)	0.81	0.83	0.53	0.47	0.30
R_{cullis}[b] (centric)	0.78	0.82	0.83	0.94	0.93
Resolution	3.5 Å	3.5 Å	3.5 Å	3.3 Å	3.5 Å
R_{merge}[c]	7.7(22.3)	7.2(24.6)	7.2(22.6)	4.4(23.2)	11.2(35.0)
Completeness[d]	73.0%	77.7%	78.3%	62.3%	73.7%
Completeness[e]	95.6%	97.0%	97.3%	91.2%	96.1%
Figure of merit	0.5662 for 7545 reflections to 5 Å				

PCMBS, p-Cl-mercuriphenylsulfonic acid; UAc, uranylacetate; PP, phasing power (phasing power and R_{cullis} up to 5 Å resolution).
[a] The PCMBS derivative was obtained from a RanP210C mutant complex.
[b] $R_{cullis} = \sum_h|F_{PH,obs}(h) - F_{PH,calc}(h)|/\sum_h|F_{PH,obs}(h) - F_P|$
[c] $R_{merge} = \sum_h\sum_i|I(h) - I_i(h)|/\sum_h\sum_i I_i(h)$, where $I_i(h)$ and I(h) are the ith and mean measurements of reflection h, respectively; values in parentheses for outer resolution shell (in %).
[d] To maximum resolution of derivatives.
[e] To 5 Å.

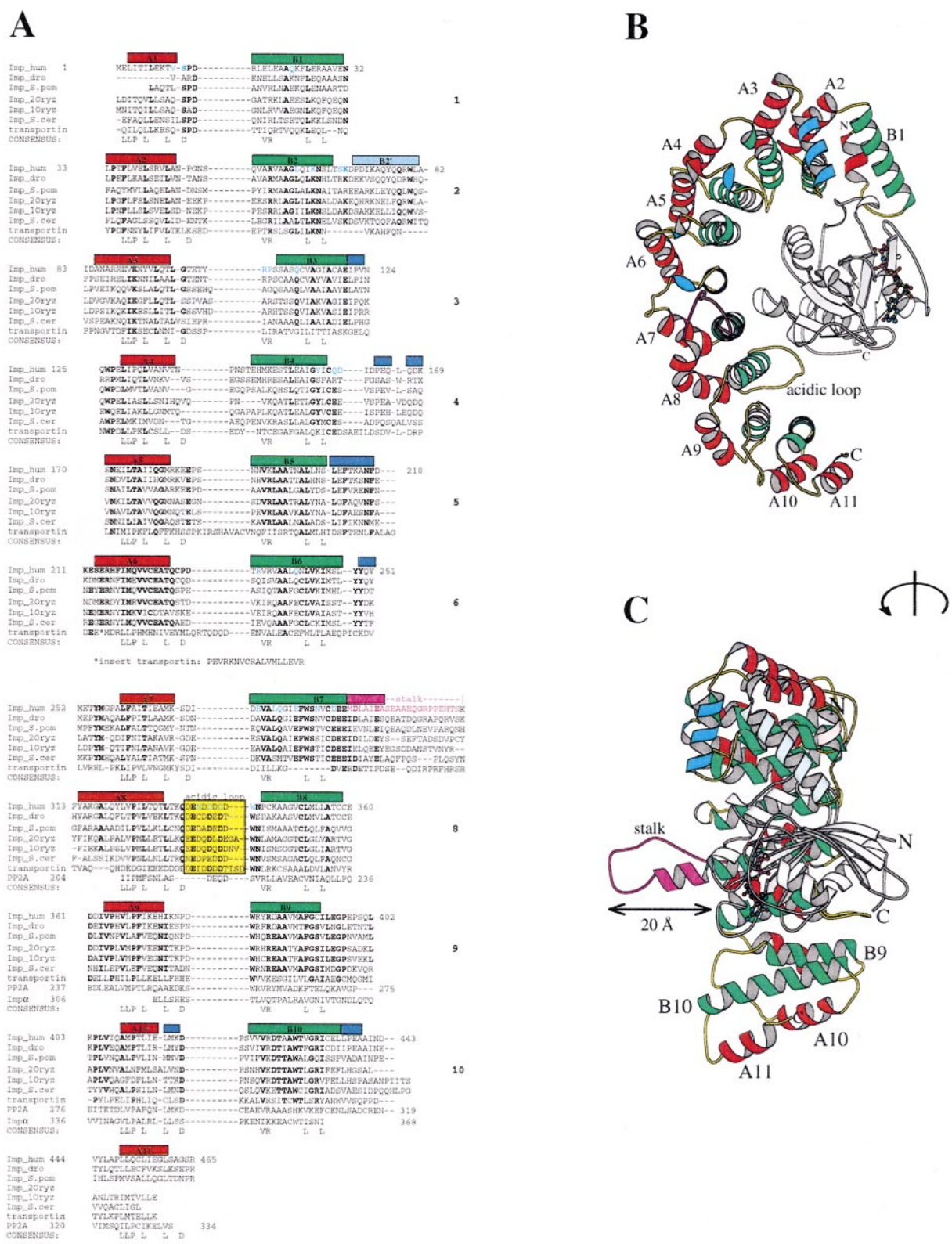

Figure 1. Primary, Secondary, and Tertiary Structure of Impβ

(A) Sequence alignment and secondary structure assignment (DSSP, Kabsch and Sander, 1983) of Impβ from various species, aligned with transportin and, where possible, the regulatory subunit of phosphatase 2A and Impα. Each repeat consists of the helices A (marked in red) and B (green); additional helices are light blue (α helix B2′) and dark blue (3^{10} helices). Residues conserved in at least 5 of the 7 import receptors (including transportin) are highlighted in bold. Also shown is the HEAT repeat consensus motif (Andrade and Bork, 1995). The GenBank accession numbers of the Impβ sequences shown are as follows: *Drosophila*, spO18388; *S. pombe*, spO13846; *Oryza sativa*, dbjBAA34862 (isoform 2); *Oryza sativa*, dbjBAA34861 (isoform 1), *S. cerevisiae*, spQ06142; human transportin, gi1613834; PP2A human (PDB code 1b3u), spP30153; Impβ, *S. cerevisiae* (PDB code 1bk5), spQ02821.

(B and C) Ribbon representation of the complex of RanGppNHp with $Imp\beta_N$, highlighting the $Imp\beta_N$ fold, where the helices have the same color code as in (A); the stalk is in purple, and loops are in yellow, Ran is in gray, and the nucleotide is a ball-and-stick model. In (C), helix A1 and B1 are shown in light red and light green for clarity (MOLSCRIPT; Kraulis, 1991). The 90° rotation of the complex is indicated.

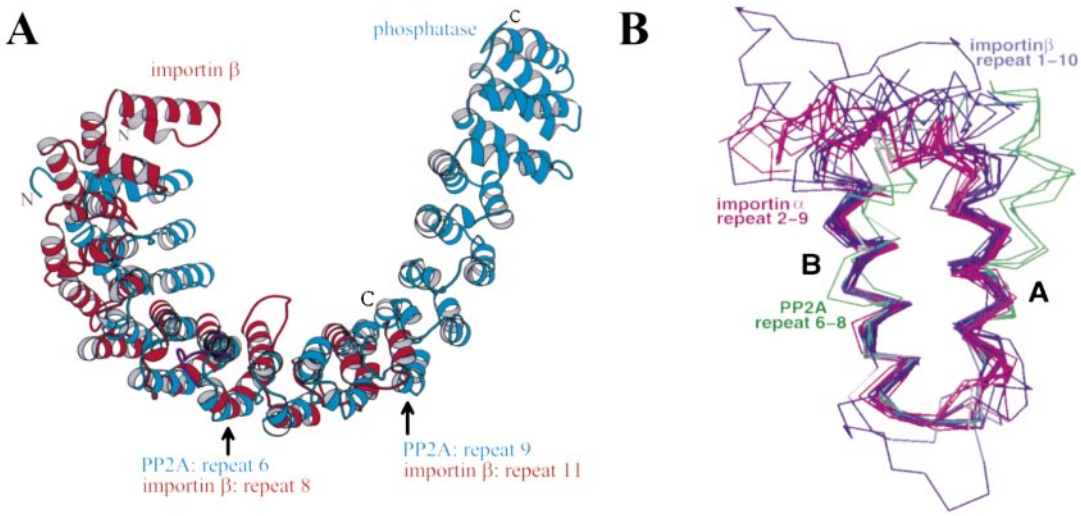

Figure 2. Comparison of the Impβ Structure with Other Structures

(A) Superimposition of the Impβ$_N$ (red) with the phosphatase subunit (blue) (Groves et al., 1999) using HEAT repeats 6–9 (residues 204–334) from the latter and 8–10 (residues 322–461) from the former (MOLSCRIPT; Kraulis, 1991).

(B) Superimposition (Cα plot) of the ten repeats of Impβ$_N$ (blue) with three HEAT repeats from PP2A (residues as above) (green) and arm repeats 2–9 of Impα (purple). The rms deviation between ten Impβ$_N$ repeats (Cα atoms, repeat 1 as reference) is 0.77–1.32 Å. Between repeat 1 from Impβ$_N$ and eight repeats from Impα and PP2A repeats, respectively, the rmsd is 0.6–082 Å and 1–2.1 Å. Figure produced with "O" (Jones and Kjeldgaard, 1997).

turn. This structure, which we term "stalk", protrudes by ~20 Å from the surface of the molecule (Figure 1C), suggesting a special, but currently unknown function. Possibly, the stalk is involved in the recognition of basic import cargoes, such as the BIB domain.

The repeat units of Impβ$_N$ are arranged together to form an irregular, crescent-shaped arch (Figure 1B). The array of helices in the last seven repeats is roughly parallel, whereas the first three are tilted with respect to the others. The first helix (A) of a repeat is located at the outer (convex) face, and the second helix (B) is located at the inner (concave) side of the arch.

HEAT and Arm Repeats

Sequence analysis had suggested that Impβ contains a series of internal repeats that bear some resemblance to HEAT repeats as well as to Armadillo (arm) motifs (Peifer et al., 1994; Andrade and Bork, 1995; Görlich et al., 1995; Figure 1A). The closest match between the regulatory A subunit of the protein phosphatase 2A (PP2A), the only HEAT repeat protein with a known 3D structure (Groves et al., 1999), and Impβ$_N$ is found between repeats 8–10 from Impβ (residues 322–461) and repeats 6–9 (residues 204–334) from PP2A (Figures 1A and 2A). The remaining repeats show a large deviation with a different curvature of the arch (Figure 2A). In contrast to Impβ$_N$, the 15 PP2A repeats have a fairly consistent architecture, length, and curvature. The individual Impβ$_N$ repeats have a similar V-shaped arrangement of helices A and B and can be superimposed very well (Figure 2B), but the relative orientation between the repeats is less regular than in PP2A. The irregular shape of Impβ is thus due to the variable intrarepeat connections. Whereas PP2A shows strong conservation of the HEAT consensus residues, which either form the hydrophobic core of the motif or the hydrophilic interrepeat connections, such residues are poorly conserved in Impβ$_N$ (Figure 1A).

Residues 373–435 from Impβ are also sequence related (Figure 1A) to a fragment of Impα (residues 306–368) that is a purely α-helical protein constructed from arm motifs. Each repeat comprises approximately 40 residues and is formed by three helices arranged roughly in the shape of a triangle (Conti et al., 1998). A superimposition of several Impα arm with Impβ$_N$ repeats (Figure 2B) shows a high local structural similarity, except that the third helix of the arm repeat is well defined in Impα but forms a less regular helix or is even nonhelical in the Impβ$_N$ repeats. Structural analysis thus shows Impβ$_N$ as an intermediate between the "two-helix" HEAT and the "three-helix" arm repeat proteins.

Structure of Ran

The structure of RanGDP alone and in complex with NTF2 (Scheffzek et al., 1995; Stewart et al., 1998) and that of RanGppNHp in complex with the Ran-binding domain 1 (RanBD1) from RanBP2 (Vetter et al., 1999a) have been determined. The structure of RanGppNHp in the Ran–Impβ$_N$ complex is very similar to the latter (rms deviation of 168 Cα atoms is 0.86 Å including the switch II region). The switch I and II regions of small GTP-binding proteins like Ras and Ran have been defined as those regions that change their structure between the GTP- and GDP-bound conformation (Milburn et al., 1990). Both RanGppNHp molecules (in complex with RanBD1 and Impβ$_N$, respectively) show the same large conformational change in the switch I region as compared to RanGDP (Figure 3A). We can thus define the switch I region of Ran as comprising residues Thr-32^{Ran} to Val-45^{Ran}. This is much longer than the corresponding switch I regions from Ras and Rho (Milburn et al., 1990; Schlichting et al., 1990; Wei et al., 1997; Ihara et al., 1998). The switch II region forms a helix in the Ran–RanBD1 complex but not in the Ran–Impβ$_N$ complex.

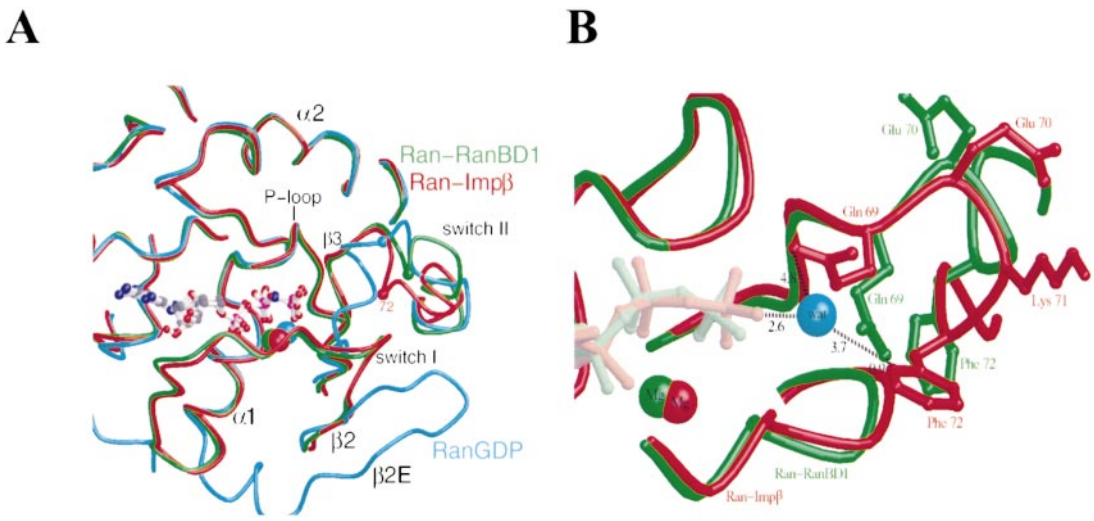

Figure 3. Structural Details of Ran in the RanGppNHp–Impβ$_N$ Complex

(A) Conformational changes of the switch I and switch II regions of Ran: RanGDP is in blue, RanGppNHp in the RanBD1 complex is in green (Vetter et al., 1999a), and RanGppNHp in the Impβ$_N$ complex is in red.

(B) The inhibition of the intrinsic GTPase of RanGTP in the RanGppNHp–Impβ$_N$ complex (red) is probably due to relocalization of the catalytic Gln69 away from the its position in the RanGppNHp–RanBD1 structure (green), as explained in the text. The catalytic water (blue sphere) is from the Ran–Impβ$_N$ structure; Mg^{2+} occupies the standard position between β,γ-phosphate in both structures (MOLSCRIPT, Raster3D, Merritt and Murphy, 1994). Superimposition uses Ran residues (Cα) from 9–176.

This is most likely due to the interaction of Impβ$_N$ with several residues of the switch II region (see below), whereas in the RanGppNHp–RanBD1 complex the RanBD1 does not contact this area. Taking the comparison between RanGDP and the Ran–Impβ$_N$ complex, the switch II region would thus be defined as residues Thr-66^{Ran} to Tyr-79^{Ran}.

The C-terminal end of Ran in the Ran–Impβ complex appears not to be structured, since no electron density is visible for the 40 C-terminal (177–216^{Ran}) residues. This correlates well with the observation that Ran's C-terminal DEDDDL motif is not only dispensable for binding to Impβ but in fact even inhibitory for fast association between Impβ and RanGppNHp (Lounsbury and Macara, 1997; J. Kuhlmann, unpublished data). In contrast, the structure of the Ran–RanBD1 complex clearly showed that the complete C-terminal extension of Ran is involved in extensive contacts with RanBD1 (Vetter et al., 1999a). Consistent with that, the removal of the C-terminal DEDDDL motif results in a 4000-fold weaker binding between RanGTP and RanBD1 (Kuhlmann et al., 1997). The disordered C terminus of Ran (residues 177–216^{Ran}) in the Ran–Impβ$_N$ complex is also evident from carboxypeptidase digests of this complex, where the last 35 residues from Ran can be cleaved off, whereas the C terminus is not accessible to carboxypeptidase in uncomplexed RanGTP (J. Kuhlmann, unpublished data).

Binding of Impβ to RanGTP not only prevents GTPase activation by RanGAP1 (Floer and Blobel, 1996; Görlich et al., 1996c), but also inhibits the intrinsic GTPase and RCC1-mediated guanine nucleotide exchange (Görlich et al., 1996c). The failure of GTPase activation by GAP and RCC1-mediated exchange is presumably due to Impβ sterically preventing the access of these factors. The inhibition of the intrinsic GTPase is more subtle, since the γ-phosphate-binding site of Ran is not in contact with Impβ. One explanation for the GTPase inhibition derives from the location of Gln-69^{Ran}; this invariant Gln residue (Q61 in Ras) plays a crucial role in the catalysis of the intrinsic and GAP-mediated GTP hydrolysis. It stabilizes the transition state of the reaction by hydrogen bonding both the attacking nucleophile (a water molecule) and an oxygen of the γ-phosphate (Privé et al., 1992; Rittinger et al., 1997; Scheffzek et al., 1997; Nassar et al., 1998). An inspection of the active site of Ran in the RanGppNHp–Impβ complex shows the putative nucleophilic water molecule at a distance of 3.4 Å to the γ-phosphate and 2.6 Å to one of the phosphate oxygens (Figure 3B), which is very similar to the RasGppNHp structure (Pai et al., 1990). However, the relevant Gln-69^{Ran} is pointing away from the nucleophilic water, explaining the GTPase inhibition. The repositioning of the crucial Gln-69^{Ran} is probably caused by Phe-72^{Ran}. Due to a potential steric clash with Trp-104 from Impβ$_N$, Arg-76^{Ran} moves out of its position in the Ran–RanBD1 complex, which in turn relocates Phe-72^{Ran} close to the position occupied by Gln-69^{Ran} in the RanBD1 complex (Figure 3B). Thus, Impβ inhibits the GTPase reaction by disturbing the GTPase active site.

The Complex

Ran Contact Regions

Binding assays with Impβ fragments have shown that the first 364 residues of Impβ are sufficient for high-affinity binding to RanGTP and that an N-terminal 343-residue fragment is unable to bind significantly (Kutay et al., 1997b). Furthermore, N-terminal deletion of 10 or 44 residues severely impairs or, respectively, completely prevents Ran binding (Chi et al., 1997; Kose et al., 1997; Kutay et al., 1997b). These observations are corroborated by the structure of the complex (Figures 4A and

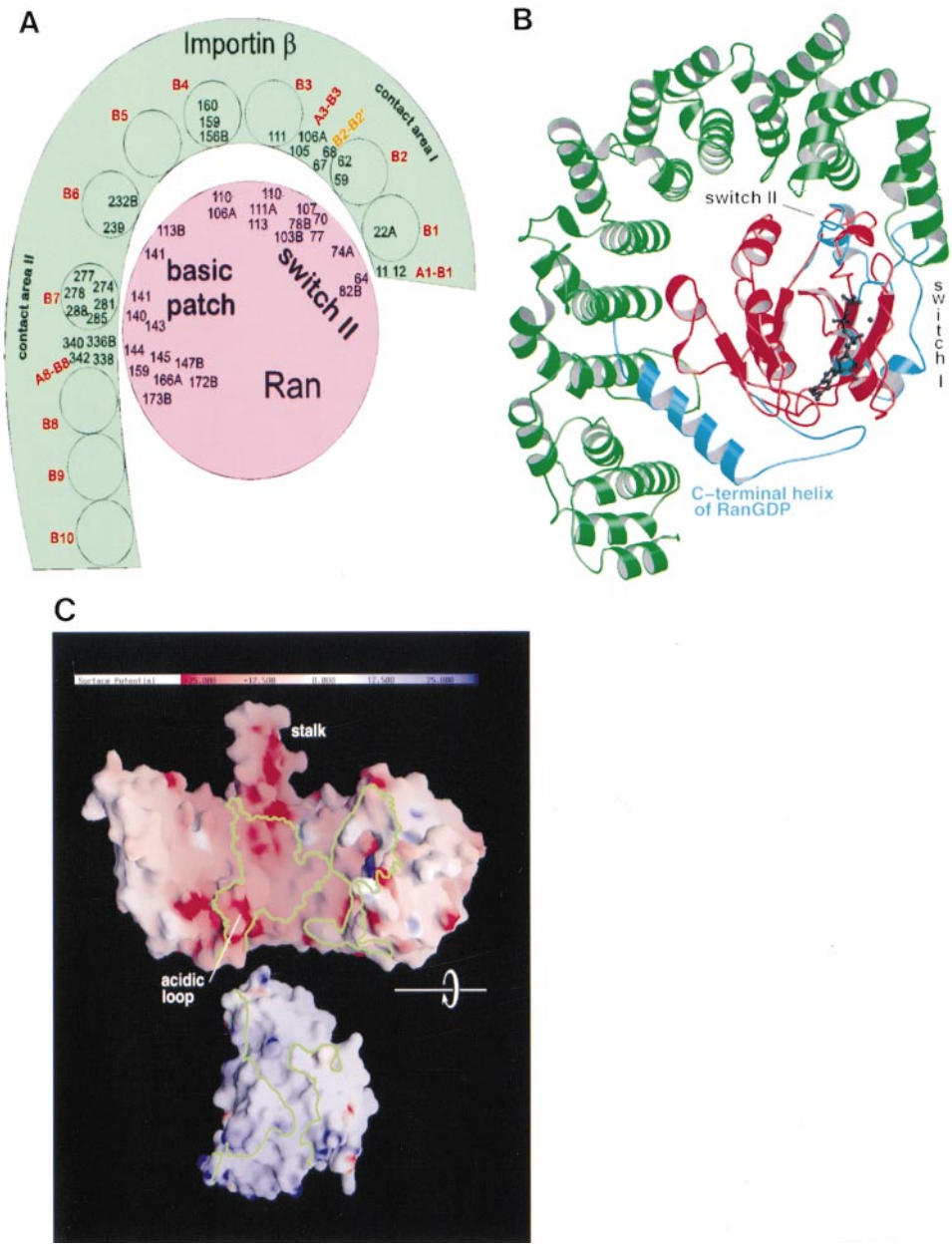

Figure 4. Structure of the Complex

(A) Schematic representation of the structure of the complex, indicating the contacts of residues on Impβ with those of Ran. Interactions found in only one of the two molecules have an additional A,B identifier on the residue number. Open circles in $Imp\beta_N$ indicate the position of the B helices of the repeats with their numbers in red.

(B) Ribbon representation of the complex with Ran in red, Impβ in green, superimposed with RanGDP in blue to highlight the potential clashes in switch I and the C-terminal end. GppNHp and Mg^{2+} are shown as black ball-and-stick models.

(C) Electrostatic surface potential of Impβ and RanGppNHp in and close to the interface (GRASP; Nicholls et al., 1991). The 180° rotation of Ran is indicated.

4B). Ran is located in the concave part of the irregular crescent formed by Impβ, forming two major areas of contact on both ends of the crescent, whereas the middle part is somewhat detached and involved in only a few contacts. Contacting residues in molecules A and B are slightly different and are marked accordingly (Figure 4A). The first contact area involves (1) helix B1 and the A1/B1 turn of Impβ interacting with residues 64^{Ran}, 74^{Ran}, and 82^{Ran} (switch II region), (2) helix B2 and the B2/B2′ turn interacting with 70^{Ran}, $77–78^{Ran}$, 103^{Ran}, and 107^{Ran}, and (3) the turn between A3 and B3 and the beginning of B3 interacting with 110^{Ran}, 111^{Ran}, and 113^{Ran} (C-terminal end of the $\alpha3^{Ran}$). The second area involves residues from helix B7 and the highly conserved acidic A8/B8 loop, which contacts Ran residues $140–147^{Ran}$ located in the $\alpha4$-$\alpha5$ area as well as residues 159^{Ran}, 166^{Ran}, and $172–173^{Ran}$. The total buried accessible surface is very large, with an average value for the two complexes of

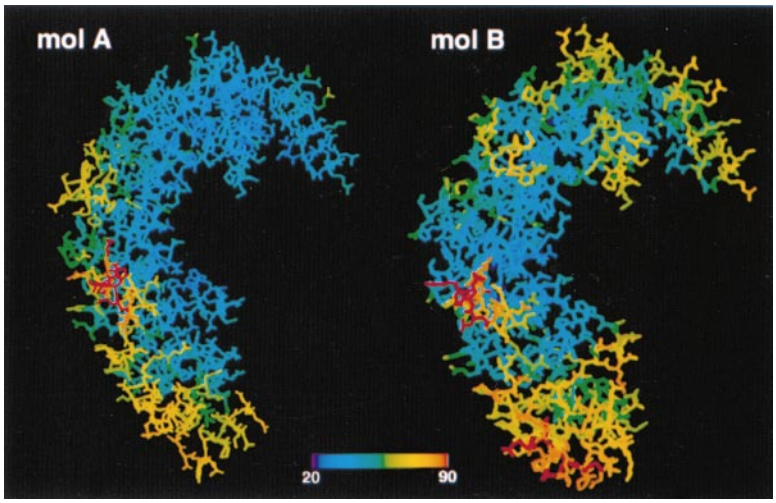

Figure 5. Flexibility of Impβ

B factor representation of the two Impβ molecules in the asymmetric unit of the crystal with a color code, where red indicates high B factors and blue indicates low B factors. This indicates the different flexibilities in the two molecules, both inside and outside the Ran interface.

3583 Å^2. There are 23 water molecules buried in the interface of molecule A, 19 of which mediate hydrogen bonds between Ran and Impβ$_N$. The structure explains the lower affinities for RanGTP of N-terminally truncated Impβ mutants: residues 11, 12, and 22 from the first repeat are directly involved in interactions. Deleting 44 residues eliminates the entire first repeat, and removal of ten residues is most likely disruptive for folding. Deleting residues of Impβ after amino acid 343 would destroy repeat 8, which is close to contact area 2.

Switch I Region of Ran

The switch I region of other Ras-like proteins is directly involved in the interaction of these proteins with their effectors, examples being complexes of Rap1A with the Ras-binding domain of c-Raf-1 (Nassar et al., 1995, 1996), Ras with the Ras-binding domain of Ral-GDS (Huang et al., 1998; Vetter et al., 1999b), and the Rab–Rabphilin complex (Ostermeier and Brunger, 1999). In contrast, the switch I region of Ran, although very close to the first repeat of Impβ, is not directly involved in the complex formation. Nevertheless, residues from Impβ are sufficiently close to prevent the effector loop from switching into the GDP conformation. This is shown in a superposition of the structure of RanGDP with the RanGppNHp–Impβ$_N$ complex (Figure 4B). The conformation of the switch I region in RanGDP would sterically hinder Impβ binding in the area of the first repeat and explains why Impβ binds RanGTP so much more strongly than RanGDP. In addition, the C terminus of RanGDP (residues 203–216^{Ran}) would clash with Impβ in repeats 7 and 8 (Figure 4B). One can thus conclude that even though switch I and the C terminus of RanGppNHp do not contact Impβ directly, they regulate complex formation by sterically inhibiting Impβ binding to RanGDP. The K_D for the formation of the RanGTP–Impβ complex has been determined to be 0.6 nM (Görlich et al., 1996c), whereas the K_D for RanGDP, too low to be measured accurately, is estimated to be above 5–10 μM (J. Kuhlmann, unpublished data). Assuming no major change in the conformation of Impβ, this huge difference in affinity thus gives an idea about the energetic cost (at least 22 kJ/mol) for changing the structures of the switch I region, switch II region, and the C terminus of Ran.

Switch II Region of Ran

The contact area 1 is predominantly formed by Ran residues 64, 70, 74, 77, 78, and 82 from switch II, which mediate hydrophilic and hydrophobic interactions with Impβ$_N$ residues 11, 12, 22, 59, 62, 67, and 68 from helices B1 and B2. The conformation of switch II of RanGppNHp is quite different between the RanBD1 complex and the Impβ$_N$ complex. One of the triggers for this conformational change might be Leu-75^{Ran}, which becomes localized into a mostly hydrophobic pocket formed by residues Thr-10, Leu-18, and Gln-22 from Impβ. This pulls Arg-76^{Ran} out of the Ran core, which now forms a salt bridge with Glu-70^{Ran} that in turn interacts with Ser-67^{Ran}. In addition, the salt bridge between Asp-77^{Ran} and Arg-110^{Ran} is broken in the Impβ$_N$–Ran complex, thus allowing the arginine to establish a number of contacts with Impβ$_N$.

The Basic Patch of Ran

Although the highly acidic C-terminal DEDDDL motif could not be identified in the structure of RanGDP (Scheffzek et al., 1995), it was proposed (Vetter et al., 1999a) that it might dock to a basic patch on the surface to explain the biochemical finding that this DEDDDL motif stabilizes the GDP-bound conformation of Ran (Richards et al., 1995). Although the structure of the GTP-bound form of Ran alone is not known, the DEDDDL motif in RanGTP is not accessible for antibodies (Hieda et al. 1999). In the Ran–Impβ$_N$ complex, this patch is deeply buried in the interface and residues Arg-140^{Ran}, Lys-141^{Ran}, Asn-143^{Ran}, Lys-159^{Ran}, and Arg-166^{Ran} interact with an area of overall opposite charge involving residues Glu-274, Gln-278, Glu-281, Asn-285, and Asp-288 as well as Asn-336, Asp-338, and Asp-340 from helix B7 and the turn between A8 and B8, respectively, in contact area II (Figure 4A). Glu-281 is part of the ^{281}EFWS^{284} motif, which is highly conserved among all β-importins but not transportin (Figure 1A). Residues Phe-282 and Trp-283 stabilize the hydrophobic core of Impβ$_N$, whereas Glu-281 contacts Arg-140^{Ran} and Lys-141^{Ran}.

Asp-340 is part of the acidic loop between A8 and B8 (residues 334–341) in which seven out of eight residues

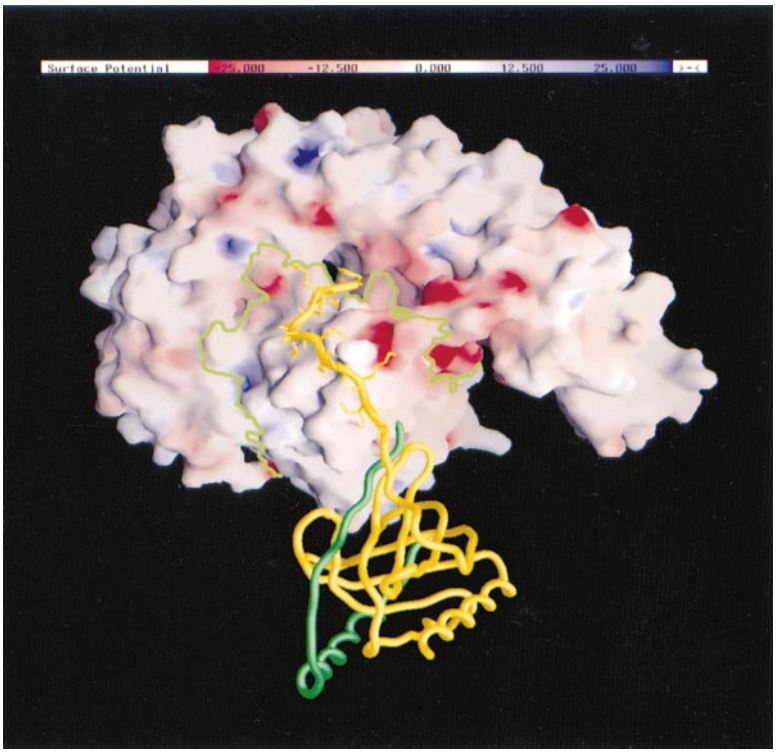

Figure 6. Model of the Ternary Ran–RanBD1–Impβ Complex, Obtained by Superimposition of RanGppNHp from Both Complexes

The Ran–Impβ complex is shown as surface and RanBD1 as a yellow worm plot, with side chains of the N-terminal end only. The C-terminal end of Ran (in green) embraces RanBD1. The outline of Ran in the Ran–Impβ complex is indicated by the green line. The most N-terminal acidic end of RanBD1 was not visible in the Ran–RanBD1 complex and is not shown here. It would be located close to the hole located in the middle of the Ran–Impβ interface (GRASP).

are acidic, and which is conspicuously similar to the DEDDDL^{Ran} motif. As mentioned above, a possible competition between the DEDDDL motif and Impβ for the basic patch of Ran is consistent with the biochemical finding that the DEDDDL motif is inhibitory for Impβ association to Ran (J. Kuhlmann, unpublished data). Trp-342 at the end of this loop is well conserved in Impβ and transportin, apparently crucial for the interaction with Ran and involved in forming the interface. The acidic loop is located on the opposite side of the protruding stalk following helix B7, and its overall negative charge is highly conserved between Impβ and transportin. That charges are important for the interaction between Impβ$_N$ and Ran can be clearly seen in Figure 4C, where the charge complementarity of the extremely negatively charged interface of Impβ$_N$ and the basic Ran surface is shown. The negative charges of Impβ$_N$ are concentrated in the area contacted by Ran, whereas the back, top, and bottom are much less charged. In addition to the interface, the protruding stalk is also highly negatively charged.

Flexibility of Impβ and Cargo Binding

The difficulty of finding isomorphous data sets during the X-ray data collection and the incomplete noncrystallographic symmetry between the two complexes in the asymmetric unit were a hint for intrinsic flexibility of the molecule. This is corroborated by comparing the temperature factors of the two Impβ molecules from the asymmetric unit of the crystal (Figure 5). Particularly high temperature factors of up to 90 Å^2 are found for the protruding stalk (residues 291–311) and the C-terminal end of molecule B of Impβ$_N$. In addition we find that in the two complexes the details of the molecular interaction between Ran and Impβ$_N$ vary considerably. With a cut-off limit of 3.5 Å, 24 out of 96 interactions are present in one complex but missing in the other (Figure 4A). This apparent flexibility of Impβ itself is most likely crucial for the interaction of Impβ with its binding partners. The fact that the interacting proteins bind to Impβ in a RanGTP-sensitive manner, and that at least in the case of Impα these binding sites are in different parts of the molecule, indicates that the structural changes in Impβ caused by RanGTP or cargo binding might be quite global.

Besides Ran, the Impβ 1–462 fragment can directly interact with Imp7, with components of the NPC such as Nup-153 and with cargo proteins containing the BIB domain, but does not measurably bind Impα (Kose et al., 1997; Kutay et al., 1997b; Jäkel and Görlich, 1998; Shah et al., 1998). The BIB domain comprises 43 residues, 30 of which are Lys, Arg, or His, with an isoelectric point of 12. Although the location of only the Ran-binding site has been determined here, the structure of Impβ$_N$ shows a number of surface-exposed acid patches that could be involved in BIB binding, the most conspicuous of which is the protruding stalk (Figure 4C).

Model of the Ran–Impβ Interaction with Ran–RanBD

Although hydrolysis of the Ran-bound GTP can in principle be accomplished by RanGAP, the disassembly of transport receptor–RanGTP complexes in the cytoplasm additionally requires RanBP1 or a RanBP1 homology domain (RanBD) from RanBP2 (Bischoff and Gör-

lich, 1997; Floer et al., 1997; Lounsbury and Macara, 1997). For RanGAP to induce the irreversible termination of nuclear export via GTP hydrolysis, the transport receptors need to be dissociated from Ran, as they block RanGAP catalysis, whereas the RanBPs in fact stimulate hydrolysis. The stimulation of dissociation of RanGTP transport receptor complexes by RanBP1 is qualitatively and/or quantitatively different for various receptors. In the case of CAS, RanBP1 is sufficient to dissociate CAS from Ran (Bischoff and Görlich, 1997), whereas in the case of Impβ, the addition of Impα is required for disassembly (Bischoff and Görlich, 1997; Floer et al., 1997).

Disassembly most likely requires an intermediate complex where Ran simultaneously contacts the transport receptor and RanBD. In the case of Impβ, this intermediate can be isolated and is actually quite stable (Chi et al., 1996; Görlich et al., 1996c; Lounsbury and Macara, 1997). A model for this ternary complex can be derived from the structural studies, as the Ran–Impβ$_N$ and the Ran–RanBD1 complexes can be superimposed on RanGppNHp (Figure 6). This model, in which RanBD1 has no contact to Impβ at all, very nicely confirms the biochemical finding that a stable ternary complex can exist. How could RanBP1 (or the RanBDs of RanBP2) induce disassembly of the receptor–RanGTP complexes? As shown here, the C-terminal end of Ran shows no interaction with Impβ. Consequently, as the C-terminal end is required for tight binding to RanBD1, RanBDs might thus recognize and capture the loosely bound or nonbound C-terminal end of Ran in the Ran–Impβ$_N$ complex, wrapping it around itself. In doing so they form a heterotrimeric complex as shown by the model of the Ran–RanBD1–Impβ$_N$ complex (Figure 6). Although we do not understand at the present time how dissociation is induced, it might involve the acidic N terminus of RanBP proteins (yellow extension in Figure 6), which in our model is located close to the hole in the Ran–Impβ complex and might end up binding to the basic patch of Ran as suggested for the Ran–RanBD1 complex (Vetter et al., 1999a). This basic patch is located close to the hole between Ran and Impβ$_N$ in the complex (Figure 6).

Conclusions

The structure of the Impβ fragment in complex with RanGppNHp shows that Ran uses its switch II region and also the α3, α4/β6/α5 region for binding. Switch I and the C-terminal residues 177–216 are not directly involved in the interface but are nevertheless important determinants for the specificity of binding. Impβ$_N$ consists of "two-helix" motifs similar to HEAT repeats, which, however, structurally resemble the "three-helix" Armadillo repeat. The many structural differences between the two molecules in the asymmetric unit, the different temperature factors of the two Impβ molecules, and the irregularity of the interrepeat connections suggest that Impβ is a rather flexible molecule. This flexibility might be important for regulation of the interactions of Impβ with its various ligands by RanGTP. The comparison of the structures of RanGppNH–RanBD1 (Vetter et al., l999a) with the RanGppNH–Impβ$_N$ complex confirms that the binding sites are nonoverlapping and hints at a possible mechanism by which RanBDs dissociate Ran from Ran–transport receptor complexes, which has to be verified by biochemical experiments. Structural studies involving Impβ–cargo and exportin–Ran–cargo complexes need to be done before we can fully understand the allosteric regulation via Ran that occurs during cargo transport in and out of the nucleus. An important step in that direction, however, has been achieved with the structure reported here.

Experimental Procedures

Protein Preparation

Wild-type and the mutant P210C Ran protein were prepared as described (Kuhlmann et al. 1997). A His-tagged construct of Impβ 1–462 (Kutay et al. 1997b) was expressed from *E. coli* strain BL 21 (DE 3), induced by 100 μM IPTG overnight, lysed in a microfluidizer, and purified over a nickel-chelate column. Nucleotide exchange of GDP bound to Ran with the nonhydrolyzable GTP analog GppNHp was achieved by incubating RanGDP with a 2-fold excess of GppNHp and 10 U of alkaline phosphatase per milligram of protein for 2 hr at room temperature in 200 mM ammonium sulfate, 10 mM EDTA (pH 7.0), 50 mM potassium phosphate buffer (pH 7.0), 5 mM $MgCl_2$, 150 mM KCl, and 5 mM DTE. Because of the limited yield of RanGppNHp (~80%), complexes with Impβ were formed with a 2-fold excess of Ran and purified over a gel filtration column.

Ran labeled with selenomethionine was prepared as described but with additional 20 mM DTE present in all buffers. The cells were grown according to the protocol of Hendrickson et al. (1990).

Crystallographic Analysis

Crystals were grown from 9.5% PEG 4000, 110 mM calcium acetate, 100 mM MES buffer (pH 6.0), 0.5% dioxane. The cryosolution consisted of 10% PEG 4000, 20% PEG 400, 100 mM MES 6.0, and 100 mM calcium acetate. The crystals had to be slowly transferred into drops with stepwise increasing concentrations of PEG 400, since they were very fragile and tended to crack very easily.

A native data set was collected at the MPG beamline BW6 at DESY, Hamburg on a MAR scanner (18 cm plate) at a wavelength of 1.1 Å and a temperature of 100 K, and the data were processed with XDS (Kabsch, 1993). The monoclinic crystals with two complexes in the asymmetric unit, space group $P2_1$ and a unit cell of a = 65.7 Å, b = 108.9 Å, c = 114.0 Å, β = 100.6 diffracted to better than 2.3 Å.

The heavy atom data sets were collected at room temperature on a rotating anode equipped with a HiStar area detector from crystals grown under slightly different conditions (+0.5% Tween 20, +50 mM sucrose). These conditions greatly improved the size, reproducibility, and isomorphism of the crystals, which was crucial for the heavy atom search. Soaks were in 1–30 mM heavy atom salt solutions for 5 min to 15 hr. To circumvent nonisomorphism problems, derivative data collected at room temperature were scaled to four different native data sets also collected at room temperature, and the scaling with the lowest R factor was selected. This procedure was crucial in finding a derivative (Table 2). The selenomethionine derivative was very useful in locating the initial position of the Ran moiety.

The initial MIR map at 5 Å was not readily interpretable. Subsequent averaging between the two complexes in the asymmetric unit combined with solvent flattening, histogram matching, and phase extension to 3.2 Å (program DM, CCP4 package [CCP4, 1994]) improved the map tremendously and allowed building of the backbone of Impβ (using "O"; Jones and Kjeldgaard, 1997) as well as fitting and rebuilding of the Ran molecules. The partial model was then carefully fitted to the high-resolution cryo data set by extensive rigid body fitting (program CNS, Brunger et al., 1998). The initial correlation was quite low due to movements of the α helices relative to each other when comparing the room temperature to the cryo data set. A similar helix movement was probably responsible for

the nonisomorphism problems during the heavy atom search. During refinement, the initial NCS symmetry used for averaging had to be released in a stepwise fashion in order to decrease the free R factor below 42%. In the last cycles of the refinement, each repeat was separately constrained and finally completely released. The free R factor was carefully monitored during this procedure. Due to a disulfide bridge between Cys-455 in molecule A and a symmetry-related Cys-436, the C terminus of this molecule is ordered. In molecule B, the bridge is between Cys-436 and the symmetry-related Cys-455. The two major sites of the best mercury derivative (PCMBS, Table I) are bound to Cys-436 of molecule A and Cys-455 of molecule B.

The final model contains 312 water molecules and has an R factor of 24.6% and a free R factor of 27.2% with excellent geometry (Table 1). Regions with weak density are 183–184, 302–309, 398–408, and 441–459 in molecule A and 299–305, 333–337, and 378–379 in molecule B.

The Ramachandran plot shows 99.1% of all residues in allowed or additional allowed regions. The nine residues in unfavorable regions have weak density (especially those in the stalk of molecule A). An exception is Arg-76^{Ran} in both Ran molecules where the unusual conformation seems to be forced by the surrounding residues.

Acknowledgments

We thank Doro Vogt for expert technical assistance, the staff from the MPG-ASBM BW6 beam line at DESY/Hamburg for help in the synchroton data collection, Jürgen Kuhlmann for continuous discussions, and Oliver Müller and Nicolas Nassar for crystallization conditions of the uncomplexed Impβ fragment.

Received April 14, 1999; revised May 12, 1999.

References

Adam, E.J.H., and Adam, S.A. (1994). Identification of cytosolic factors required for nuclear location sequence-mediated binding to the nuclear envelope. J. Cell Biol. *125*, 547–555.

Andrade, M.A., and Bork, P. (1995). HEAT repeats in the Huntington's disease protein. Nat. Genet. *11*, 115–116.

Bischoff, F.R., and Görlich, D. (1997). RanBP1 is crucial for the release of RanGTP from importin beta-related nuclear transport factors. FEBS Lett. *419*, 249–254.

Bischoff, F.R., and Ponstingl, H. (1991a). Catalysis of guanine nucleotide exchange on Ran by the mitotic regulator RCC1. Nature *354*, 80–82.

Bischoff, F.R., and Ponstingl, H. (1991b). Mitotic regulator protein RCC1 is complexed with a nuclear ras-related polypeptide. Proc. Natl. Acad. Sci. USA *88*, 10830–10834.

Bischoff, F.R., Klebe, C., Kretschmer, J., Wittinghofer, A., and Ponstingl, H. (1994). RanGAP1 induces GTPase activity of nuclear ras-related Ran. Proc. Natl. Acad. Sci. USA *91*, 2587–2591.

Bischoff, F.R., Krebber, H., Smirnova, E., Dong, W.H., and Ponstingl, H. (1995). Coactivation of RanGTPase and inhibition of GTP dissociation by Ran GTP binding protein RanBP1. EMBO J. *14*, 705–715.

Brunger, A.T., Adams, P.D., Clore, G.M., Delano, W.L., Gros, P., Grosse-Kunstleve, R.W., Jiang, J.-S., Kuszewski, J., Nilges, M., Pannu, N.S., et al. (1998). Crystallography and NMR system: a new software system for macromolecular structure determination. Acta Crystallogr. D *54*, 905–921.

Chi, N.C., Adam, E.J., and Adam, S.A. (1995). Sequence and characterization of cytoplasmic nuclear protein import factor p97. J. Cell Biol. *130*, 265–274.

Chi, N.C., Adam, E.J.H., Visser, G.D., and Adam, S.A. (1996). RanBP1 stabilizes the interaction of Ran with p97 in nuclear protein import. J. Cell Biol. *135*, 559–569.

Chi, N.C., Adam, E.J.H., and Adam, S.A. (1997). Different binding domains for Ran-GTP and Ran-GDP/RanBP1 on nuclear import factor p97. J. Biol. Chem. *272*, 6818–6822.

Collaborative Computational Project, Number 4. (1994). The CCP4 suite: programs for protein crystallography. Acta Crystallogr. D *50*, 760–763.

Conti, E., Uy, M., Leighton, L., Blobel, G., and Kuriyan, J. (1998). Crystallographic analysis of the recognition of a nuclear localization signal by the nuclear import factor karyopherin alpha. Cell *94*, 193–204.

Drivas, G.T., Shih, A., Coutavas, E., Rush, M.G., and D'Eustachio, P. (1990). Characterization of four novel ras-like genes expressed in a human teratocarcinoma cell line. Mol. Cell. Biol. *10*, 1793–1798.

Floer, M., and Blobel, G. (1996). The nuclear transport factor karyopherin β binds stoichiometrically to Ran-GTP and inhibits the Ran GTPase activating protein. J. Biol. Chem. *271*, 5313–5316.

Floer, M., Blobel, G., and Rexach, M. (1997). Disassembly of RanGTP-karyopherin beta complex, an intermediate in nuclear protein import. J. Biol. Chem. *272*, 19538–19546.

Fornerod, M., Ohno, M., Yoshida, M., and Mattaj, I.W. (1997a). CRM1 is an export receptor for leucine rich nuclear export signals. Cell *90*, 1051–1060.

Fornerod, M., van Deursen, J., van Baal, S., Reynolds, A., Davis, D., Murti, K.G., Fransen, J., and Grosveld, G. (1997b). The human homologue of yeast CRM1 is in a dynamic subcomplex with CAN/Nup214 and a novel nuclear pore component Nup88. EMBO J. *16*, 807–816.

Görlich, D., Prehn, S., Laskey, R.A., and Hartmann, E. (1994). Isolation of a protein that is essential for the first step of nuclear protein import. Cell *79*, 767–778.

Görlich, D., Kostka, S., Kraft, R., Dingwall, C., Laskey, R.A., Hartmann, E., and Prehn, S. (1995). Two different subunits of importin cooperate to recognize nuclear localization signals and bind them to the nuclear envelope. Curr. Biol. *5*, 383–392.

Görlich, D., Henklein, P., Laskey, R.A., and Hartmann, E. (1996a). A 41 amino acid motif in importin alpha confers binding to importin beta and hence transit into the nucleus. EMBO J. *15*, 1810–1817.

Görlich, D., Kraft, R., Kostka, S., Vogel, F., Hartmann, E., Laskey, R.A., Mattaj, I.W., and Izaurralde, E. (1996b). Importin provides a link between nuclear protein import and U snRNA export. Cell *87*, 21–32.

Görlich, D., Pante, N., Kutay, U., Aebi, U., and Bischoff, F.R. (1996c). Identification of different roles for RanGDP and RanGTP in nuclear protein import. EMBO J. *15*, 5584–5594.

Görlich, D., Dabrowski, M., Bischoff, F.R., Kutay, U., Bork, P., Hartmann, E., Prehn, S., and Izaurralde, E. (1997). A novel class of RanGTP binding proteins. J. Cell Biol. *138*, 65–80.

Groves, M.R., Hanlon, N., Turowski, P., Hemmings, B.A., and Barford, D. (1999). The structure of the protein phosphatase 2A PR65/A subunit reveals the conformation of its 15 tandemly repeated HEAT motifs. Cell *96*, 99–110.

Henderson, B.R., and Percipalle, P. (1997). Interactions between HIV Rev and nuclear import and export factors: the Rev nuclear localisation signal mediates specific binding to human importin-beta. J. Mol. Biol. *274*, 693–707.

Hendrickson, W.A., Horton, J.R., and LeMaster D.M. (1990). Selenomethionyl proteins produced for analysis by multiwavelength anomalous diffraction (MAD): a vehicle for direct determination of three-dimensional structure. EMBO J. *9*, 1665–1672.

Hieda, M., Tachibana, T., Yokoya, F., Kose, S., Imamoto, N., and Yoneda, Y. (1999). A monoclonal antibody to the COOH-terminal acidic portion of Ran inhibits both the recycling of Ran and nuclear protein import in living cells. J. Cell Biol. *144*, 645–655.

Hillig, R., Renault, L., Vetter, I.R., Drell, T., Nassar, N., Wittinghofer, A., and Becker, J. (1999). The crystal structure of Rna1p—a new fold for a GTPase-activating protein. Mol. Cell, in press.

Huang, L., Hofer, F., Martin, G.S., and Kim, S.-H. (1998). Structural basis for the interaction of Ras with RalGDS. Nat. Struct. Biol. *5*, 422–426.

Ihara, K., Muraguchi, S., Kato, M., Shimizu, T., Shirakawa, M., Kuroda, S., Kaibuchi, K., and Hakoshima, T. (1998). Crystal structure

of human RhoA in a dominantly active form complexed with a GTP analogue. J. Biol. Chem. *273*, 9656–9666.

Imamoto, N., Shimamoto, T., Kose, S., Takao, T., Tachibana, T., Matsubae, M., Sekimoto, T., Shimonishi, Y., and Yoneda, Y. (1995). The nuclear pore targeting complex binds to nuclear pores after association with a karyophile. FEBS Lett. *368*, 415–419.

Izaurralde, E., Kutay, U., von Kobbe, C., Mattaj, I.W., and Görlich, D. (1997). The asymmetric distribution of the constituents of the Ran system is essential for transport into and out of the nucleus. EMBO J. *16*, 6535–6547.

Jäkel, S., and Görlich, D. (1998). Importin beta, transportin, RanBP5 and RanBP7 mediate nuclear import of ribosomal proteins in mammalian cells. EMBO J. *17*, 4491–4502.

Jäkel, S., Albig, W., Kutay, U., Bischoff, F.R., Schwamborn, K., Doenecke, D., and Görlich, D. (1999). The importin beta/importin 7 heterodimer is a functional nuclear import receptor for histone H1. EMBO J., in press.

Jones, T.A., and Kjeldgaard, M. (1997). Electron-density map interpretation. Methods Enzymol. *277*, 173–208.

Kabsch, W. (1993). Automatic processing of rotation diffraction data from crystals of initially unknown symmetry and cell contents. J. Appl. Crystallogr. *26*, 795–800.

Kabsch, W., and Sander, C. (1983). Dictionary of protein secondary structure: pattern recognition of hydrogen-bonded and geometrical features. Biopolymers *22*, 2577–2637.

Kose, S., Imamoto, N., Tachibana, T., Shimamoto, T., and Yoneda, Y. (1997). Ran-unassisted nuclear migration of a 97-kD component of nuclear pore-targeting complex. J. Cell Biol. *139*, 841–849.

Kraulis, P.J. (1991). MOLSCRIPT: a program to produce both detailed and schematic plots of protein structures. J. Appl. Crystallogr. *24*, 946–950.

Kuhlmann, J., Macara, I., and Wittinghofer, A. (1997). Dynamic and equilibrium studies on the interaction of Ran with its effector RanBP1. Biochemistry *36*, 12027–12035.

Kutay, U., Bischoff, F.R., Kostka, S., Kraft, R., and Görlich, D. (1997a). Export of importin α from the nucleus is mediated by a specific nuclear transport factor. Cell *90*, 1061–1071.

Kutay, U., Izaurralde, E., Bischoff, F.R., Mattaj, I.W., and Görlich, D. (1997b). Dominant-negative mutants of importin-beta block multiple pathways of import and export through the nuclear pore complex. EMBO J. *16*, 1153–1163.

Lounsbury, K.M., and Macara, I.G. (1997). Ran-binding protein 1 (RanBP1) forms a ternary complex with Ran and karyopherin beta and reduces Ran GTPase-activating protein (RanGAP) inhibition by karyopherin beta. J. Biol. Chem. *272*, 551–555.

Mattaj, I.W., and Englmeier, L. (1998). Nucleocytoplasmic transport: the soluble phase. Annu. Rev. Biochem. *67*, 265–306.

Melchior, F., Paschal, B., Evans, E., and Gerace, L. (1993). Inhibition of nuclear protein import by nonhydrolyzable analogs of GTP and identification of the small GTPase Ran/TC4 as an essential transport factor. J. Cell Biol. *123*, 1649–1659.

Merritt, E.A., and Murphy, M.E.P. (1994). Raster3D version 2.0. A program for photorealistic molecular graphics. Acta Crystallogr. D *50*, 869–873.

Milburn, M.V., Tong, L., DeVos, A.M., Brünger, A., Yamaizumi, Z., Nishimura, S., and Kim, S.-H. (1990). Molecular switch for signal transduction: structural differences between active and inactive forms of protooncogenic *ras* proteins. Science *247*, 939–945.

Moore, M.S., and Blobel, G. (1993). The GTP-binding protein Ran/TC4 is required for protein import into the nucleus. Nature *365*, 661–663.

Nassar, N., Horn, G., Herrmann, C., Scherer, A., McCormick, F., and Wittinghofer, A. (1995). The 2.2 Å crystal structure of the Ras-binding domain of the serine/threonine kinase c-Raf1 in complex with Rap1A and a GTP analogue. Nature *375*, 554–560.

Nassar, N., Horn, G., Herrmann, C., Block, C., Janknecht, R., and Wittinghofer, A. (1996). Ras/Rap effector specificity determined by charge reversal. Nat. Struct. Biol. *3*, 723–729.

Nassar, N., Hoffmann, G.R., Manor, D., Clardy, J.C., and Cerione, R.A. (1998). Structures of Cdc42 bound to the active and catalytically compromised forms of Cdc42GAP. Nat. Struct. Biol. *5*, 1047–1052.

Nicholls, A., Sharp, K.A., and Honig, B. (1991). Protein folding and association: insights from the interfacial and thermodynamic properties of hydrocarbons. Proteins *11*, 281–296.

Ohtsubo, M., Okazaki, H., and Nishimoto, T. (1989). The RCC1 protein, a regulator for the onset of chromosome condensation locates in the nucleus and binds to DNA. J. Cell Biol. *109*, 1389–1397.

Ostermeier, C., and Brunger, A.T. (1999). Structural basis of Rab effector specificity: crystal structure of the small G protein Rab3A complexed with the effector domain of Rabphilin-3A. Cell *96*, 363–374.

Pai, E.F., Krengel, U., Petsko, G.A., Goody, R.S., Kabsch, W., and Wittinghofer, A. (1990). Refined crystal structure of the triphosphate conformation of H-ras p21 at 1.35Å resolution: implications for the mechanism of GTP hydrolysis. EMBO J. *9*, 2351–2359.

Peifer, M., Berg, S., and Reynolds, A.B. (1994). A repeating amino acid motif shared by proteins with diverse cellular roles. Cell *76*, 789–791.

Privé, G.G., Milburn, M.V., Tong, L., DeVos, A.M., Yamaizumi, Z., Nishimura, S., and Kim, S.H. (1992). X-ray crystal structures of transforming p21 ras mutants suggest a transition-state stabilization mechanism for GTP hydrolysis. Proc. Natl. Acad. Sci. USA *80*, 3649–3653.

Radu, A., Blobel, G., and Moore, M.S. (1995). Identification of a protein complex that is required for nuclear protein import and mediates docking of import substrate to distinct nucleoporins. Proc. Natl. Acad. Sci. USA *92*, 1769–1773.

Renault, L., Nassar, N., Vetter, I., Becker, J., Klebe, C., Roth, M., and Wittinghofer, A. (1998). The 1.7 Å crystal structure of the regulator of chromosome condensation (RCC1) reveals a seven-bladed propeller. Nature *392*, 97–101.

Rexach, M., and Blobel, G. (1995). Protein import into nuclei: association and dissociation reactions involving transport substrate, transport factors, and nucleoporins. Cell *83*, 683–692.

Richards, S.A., Lounsbury, K.M., and Macara, I.G. (1995). The C terminus of the nuclear RAN/TC4 GTPase stabilizes the GDP-bound state and mediates interactions with RCC1, RAN-GAP, and HTF9A/RANBP1. J. Biol. Chem. *270*, 14405–14411.

Rittinger, K., Walker, P.A., Eccleston, J.F., Smerdon, S.J., and Gamblin, S.J. (1997). Structure at 1.65 Å of RhoA and its GTPase-activating protein in complex with a transition-state analogue. Nature *389*, 758–762.

Scheffzek, K., Klebe, C., Fritz-Wolf, K., Kabsch, W., and Wittinghofer, A. (1995). Crystal structure of the nuclear Ras-related protein Ran in its GDP-bound form. Nature *374*, 378–381.

Scheffzek, K., Ahmadian, M.R., Kabsch, W., Wiesmüller, L., Lautwein, A., Schmitz, F., and Wittinghofer, A. (1997). The Ras-RasGAP complex: structural basis for GTPase activation and its loss in oncogenic Ras mutants. Science *277*, 333–338.

Schlichting, I., Almo, S., Rapp, G., Wilson, K., Petratos, K., Lentfer, A., Wittinghofer, A., Kabsch, W., Pai, E.F., Petsko, G.A., and Goody, R.S. (1990). Time resolved X-ray structural studies on H-ras p21: identification of the conformational change induced by GTP hydrolysis. Nature *345*, 309–315.

Shah, S., Tugendreich, S., and Forbes, D. (1998). Major binding sites for the nuclear import receptor are the internal nucleoporin Nup153 and the adjacent nuclear filament protein Tpr. J. Cell Biol. *141*, 31–49.

Siomi, M.C., Eder, P.S., Kataoka, N., Wan, L., Liu, Q., and Dreyfuss, G. (1997). Transportin-mediated nuclear import of heterogeneous nuclear RNP proteins. J. Cell Biol. *138*, 1181–1192.

Stewart, M., Kent, H.M., and McCoy, A.J. (1998). Structural basis for molecular recognition between nuclear transport factor 2 (NTF2) and the GDP-bound form of the Ras-family GTPase Ran. J. Mol. Biol. *277*, 635–646.

Truant, R., and Cullen, B.R. (1999). The arginine-rich domains present in human immunodeficiency virus type 1 tat and rev function as direct importin beta-dependent nuclear localization signals. Mol. Cell. Biol. *19*, 1210–1217.

Vetter, I.R., Nowak, C., Nishimoto, T., Kuhlmann, J., and Wittinghofer, A. (1999a). Structure of a Ran-binding domain complexed with Ran bound to a GTP analogue: implications for nuclear transport. Nature *398*, 39–46.

Vetter, I.R., Linnemann, T., Wohlgemuth, S., Geyer, M., Kalbitzer, H.R., Herrmann, C., and Wittinghofer, A. (1999b). Structural and biochemical analysis of Ras-effector signaling via RalGDS. FEBS Lett., in press.

Wei, Y., Zhang, Y., Derewenda, U., Liu, X., Minor, W., Nakamoto, R.K., Somlyo, A.W., Somlyo, A.P., and Derewenda, Z.S. (1997). Crystal structure of RhoA-GDP and its functional implications. Nat. Struct. Biol. *4*, 699–703.

Weis, K., Ryder, U., and Lamond, A.I. (1996). The conserved amino-terminal domain of hSRP1 alpha is essential for nuclear protein import. EMBO J. *15*, 1818–1825.

Protein Data Bank ID Code

Coordinates for the complex have been submitted with the ID code 1ibr.